

Topological suppression of optical tunneling in a twisted annular fiber

M. Ornigotti, G. Della Valle, D. Gatti, and S. Longhi

*Dipartimento di Fisica and Istituto di Fotonica e Nanotecnologie del CNR, Politecnico di Milano,
Piazza L. da Vinci 32, I-20133 Milan, Italy*

(Received 2 July 2007; published 31 August 2007)

A classical wave-optics analog of topological (Aharonov-Bohm) suppression of tunneling in a double-well potential on a ring threaded by a magnetic flux is proposed. The optical system consists of a uniformly twisted optical fiber with a structured annular core, in which the fiber twist mimics the role of the magnetic flux in the corresponding quantum-mechanical problem. Light waves trapped in the annular core of the fiber experience an additional topological (Aharonov-Bohm) phase, which may lead to the destruction of optical tunneling at certain values of the twist rate.

DOI: [10.1103/PhysRevA.76.023833](https://doi.org/10.1103/PhysRevA.76.023833)

PACS number(s): 42.81.Qb, 03.65.Xp, 73.23.-b, 75.45.+j

I. INTRODUCTION

Tunneling of a wave function between two communicating wells of a bistable potential is a rather universal phenomenon encountered in a wide variety of quantum systems at the mesoscopic and macroscopic levels (see, for instance, Refs. [1,2]). Owing to the splitting of the ground-state energies of the double-well system, a wave initially localized in one of the two wells periodically tunnels back and forth between them in a characteristic time which is inversely proportional to the doublet energy splitting. Such a familiar dynamical behavior may be strongly modified when the system is exposed to a time-dependent driving field [2]. In particular, for a periodic driving force tunneling can be brought to a complete standstill under certain conditions, a phenomenon which is usually referred to as “coherent destruction of tunneling” (CDT) [2,3]. A related problem is that of tunneling of a quantum particle in a double-well potential constrained to move on a closed loop, such as on a ring, threaded by a magnetic flux [4]. As compared to a double well on the line, in this case there exist two different paths connecting the two wells on the closed loop and the tunneling rate is thus modified. Interestingly, when the ring is threaded by the magnetic flux, an additional Aharonov-Bohm phase appears in the wave function which can lead to tunneling suppression for certain values of the magnetic flux [4–6]. As compared to CDT, in this case tunneling suppression has a topological origin and arises as a destructive interference between different tunneling paths. Such a kind of tunneling suppression of purely topological origin has been theoretically predicted [5,6] and experimentally observed [7] in magnetic systems as a periodic quenching of the ground-state energy splitting when the applied magnetic field is increased. Instead of threading a quantum ring with a magnetic flux, the additional topological phase can be achieved by rotating the ring around its axis, the Coriolis force in the noninertial reference frame playing an analogous role of the magnetic force (see, for instance, Refs. [8,9]). In spite of the fact that these phenomena have been mostly investigated in the framework of quantum systems, they may be observed as well in classical wave optics owing to the strong similarities between quantum and optical wave phenomena (see, for instance, Refs. [10–12], and references therein). Electromagnetic analog of

tunneling enhancement and suppression in a driven bistable potential have been recently demonstrated using two engineered evanescently coupled optical waveguides [13,14], where the refractive index profile transverse to the propagation direction of light mimics the double-well potential of the corresponding quantum problem whereas the temporal evolution of the wave function is replaced by the spatial evolution of the light wave along the propagation direction. The optical analog of the motion of a quantum particle on a ring is represented by ray propagation in microstructured annular optical guides, which can be nowadays designed and fabricated thanks to the impressive advances in optical fiber technology (see, for instance, Refs. [15–17], and references therein).

In this work we theoretically propose an optical analog of *topological* quantum tunneling suppression via Aharonov-Bohm destructive interference based on a uniformly twisted structured annular-core fiber. The annular core of the fiber is designed such that light is preferentially confined to two sectors of the core and evanescent coupling of optical waves (optical tunneling) is allowed along the two paths of the ring. A topological additional phase, which mimics the Aharonov-Bohm phase induced by the magnetic flux in the corresponding quantum problem, is attained by a uniform twist of the fiber around its axis. In the twisted reference frame, optical rays experience both centrifugal and Coriolis forces (see, for instance, Ref. [18]), the latter one being analogous to the magnetic (Lorentz) force and thus responsible for the appearance of an additional topological phase. As in the untwisted fiber an initial light beam injected into one of the two high-index sectors of the annular core undergoes periodic optical tunneling as in a usual optical directional coupler, in the twisted case the spatial length of the optical tunneling varies with the twist rate ϵ , and at certain values of ϵ tunneling can be completely suppressed via destructive interference.

The paper is organized as follows. In Sec. II the basic model of light propagation in a twisted annular-core fiber with a structured core is presented and a variational analysis is used to capture the dynamics of light waves trapped in the annular core region. In Sec. III topological suppression of the tunnel splitting induced by fiber twist is discussed and the optical-quantum analogy is clarified. Numerical simulations of light propagation in the twisted annular fiber are presented

in Sec. IV, which confirm the theoretical predictions. Finally, in Sec. V the main conclusions are outlined.

II. BASIC MODEL AND VARIATIONAL ANALYSIS

A. Annular fiber model

The starting point of our analysis is provided by a rather standard model for monochromatic light propagation at frequency ω in a guiding dielectric structure with a refractive index profile $n(x, y, z)$, which describes a fiber with a structured annular core in the transverse (x, y) plane uniformly twisted along the propagation direction z with a spatial twist period Λ . In the weak guidance approximation, where the refractive index $n(x, y, z)$ weakly deviates from the substrate (cladding) index n_s , the scalar field approximation can be used (see, for instance, Refs. [19–21]) and propagation of the electric field E , in a given polarization state, is ruled by the Helmholtz equation

$$\frac{\partial^2 E}{\partial z^2} + \nabla_{\perp}^2 E + k_0^2 n^2(x, y, z) E = 0, \quad (1)$$

where $\nabla_{\perp}^2 = (\partial^2/\partial x^2) + (\partial^2/\partial y^2)$ is the transverse Laplacian, $k_0 = (\omega/c_0)$, and $\lambda = 2\pi/k_0$ is the wavelength of light in vacuum. In a rotating frame that follows the fiber twist [18], Eq. (1) takes the form

$$\left(\frac{\partial}{\partial z} - \epsilon \frac{\partial}{\partial \theta}\right)^2 E + \nabla_{\perp}^2 E + k_0^2 n^2(r, \theta) E = 0, \quad (2)$$

where (r, θ) are the polar coordinates in the rotating transverse reference frame, $\epsilon = 2\pi/\Lambda$ is the twist rate, and $\nabla_{\perp}^2 = (1/r)(\partial E/\partial r) + (\partial^2 E/\partial r^2) + (1/r^2)(\partial^2 E/\partial \theta^2)$. In our model, we consider a fiber index profile $n(r, \theta)$ which slightly deviates from that of a step-index annular-core fiber [20]; i.e., we set $n(r, \theta) = n_0(r) + \Delta n(r, \theta)$, where $n_0(r) = n_2$ for $|r-a| < \delta/2$, $n_0(r) = n_s$ for $|r-a| > \delta/2$, a and δ are the annular core radius and thickness, respectively, $(n_2 - n_s) \ll n_s$ and $|\Delta n| \ll (n_2 - n_s)$. The behavior of $\Delta n(r, \theta)$ —i.e., of the index profile increase in the annular-core region—is left undetermined at this stage and will be specified in the following.

B. Variational analysis

Propagation of light waves trapped in the annular core region can be at best captured in the limit of a narrow ring ($\delta \ll a$) by eliminating from Eq. (2) the radial part of the field and looking for an amplitude equation for the angular part solely [22]. Owing to the presence of the structured part $\Delta n(r, \theta)$ in the core region, the problem is not exactly separable and one has to resort to approximate techniques to capture the angular wave dynamics. To this aim, let us notice that Eq. (2) can be derived from the variational principle $\delta \int r dr d\theta dz \mathcal{L} = 0$ with a Lagrangian density $\mathcal{L} = \mathcal{L}(E, E^*, E_z, E_z^*, E_{\theta}, E_{\theta}^*, E_r, E_r^*)$ given by

$$\mathcal{L} = k_0^2 n^2(r, \theta) E E^* - \frac{\partial E}{\partial r} \frac{\partial E^*}{\partial r} - \frac{1}{r^2} \frac{\partial E}{\partial \theta} \frac{\partial E^*}{\partial \theta} - \left(\frac{\partial E}{\partial z} - \epsilon \frac{\partial E}{\partial \theta}\right) \left(\frac{\partial E^*}{\partial z} - \epsilon \frac{\partial E^*}{\partial \theta}\right). \quad (3)$$

Let us indicate by $E(r) = R(r) \exp(in_e k_0 z)$ the angular-invariant fundamental mode of the annular fiber for $\Delta n = 0$, where $R(r)$ is the radial mode profile and n_e the mode effective index, i.e., $(1/r)(\partial R/\partial r) + (\partial^2 R/\partial r^2) + k_0^2 n_0^2(r) R(r) = k_0^2 n_e^2 R(r)$. Let us then look for an approximate solution to Eq. (2) of the form $E(r, \theta, z) \approx R(r) f(\theta, z)$, where $f(\theta, z)$ describes the angular distribution of light waves. After setting $n^2(r, \theta) \approx n_0^2(r) + 2n_0(r)\Delta n(r, \theta)$, the evolution equation for $f(\theta, z)$ is given by the Euler-Lagrange equation

$$\frac{\partial \mathcal{L}_{red}}{\partial f^*} - \frac{\partial}{\partial \theta} \frac{\partial \mathcal{L}_{red}}{\partial f_{\theta}^*} - \frac{\partial}{\partial z} \frac{\partial \mathcal{L}_{red}}{\partial f_z^*} = 0 \quad (4)$$

for the reduced Lagrangian density $\mathcal{L}_{red} = \int_0^{\infty} dr r \mathcal{L}$. Assuming the normalization condition $\int_0^{\infty} dr r |R(r)|^2 = 1$, the reduced Lagrangian density reads explicitly

$$\mathcal{L}_{red} = k_0^2 [n_e^2 - 2n_e V_e(\theta)] f f^* - \frac{1}{R_0^2} \frac{\partial f}{\partial \theta} \frac{\partial f^*}{\partial \theta} - \left(\frac{\partial f}{\partial z} - \epsilon \frac{\partial f}{\partial \theta}\right) \left(\frac{\partial f^*}{\partial z} - \epsilon \frac{\partial f^*}{\partial \theta}\right), \quad (5)$$

where we have set

$$V_e(\theta) \equiv -\frac{1}{n_e} \int_0^{\infty} dr r n_0(r) \Delta n(r, \theta) |R(r)|^2 \quad (6)$$

and

$$\frac{1}{R_0^2} \equiv \int_0^{\infty} dr \frac{1}{r} |R(r)|^2. \quad (7)$$

Note that, for a narrow annulus, R_0 is close to the mean radius a of the ring fiber core. From Eq. (4) one then obtains the following evolution equation for f :

$$\left(\frac{\partial}{\partial z} - \epsilon \frac{\partial}{\partial \theta}\right)^2 f + \frac{1}{R_0^2} \frac{\partial^2 f}{\partial \theta^2} + k_0^2 [n_e^2 - 2n_e V_e(\theta)] f = 0. \quad (8)$$

III. TOPOLOGICAL SUPPRESSION OF OPTICAL TUNNELING

A. Modes of the twisted fiber and suppression of tunnel splitting

The angular modes of the twisted fiber can be derived from Eq. (8) by setting $f(z, \theta) = A(\theta) \exp(i\beta z)$, where the angular mode profile $A(\theta)$ and corresponding propagation constant β are found as eigenfunctions and eigenvalues of the equation

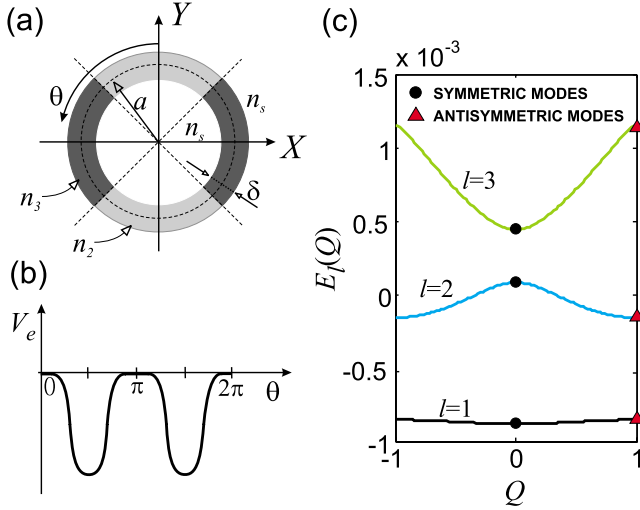


FIG. 1. (Color online) (a) Schematic of a step-index annular fiber with a four-sector core for the observation of topological suppression of optical tunneling. (b) Typical behavior of the effective double-well angular potential V_e [Eq. (6)]. For the step-index fiber of (a) the effective potential is a double square well. (c) Band diagram $E_l(Q)$ corresponding to the step-index annular fiber (parameter values are given in Sec. IV). Symmetric and antisymmetric modes correspond to the allowed values of $Q=0$ and $Q=1$ at the different band orders l , respectively.

$$\left(i\beta - \epsilon \frac{d}{d\theta}\right)^2 A + \frac{1}{R_0^2} \frac{d^2 A}{d\theta^2} + k_0^2 [n_e^2 - 2n_e V_e(\theta)] A = 0, \quad (9)$$

with the monodromy condition $A(\theta+2\pi)=A(\theta)$. Consider first the case of an untwisted fiber, corresponding to $\epsilon=0$, so that Eq. (9) reads

$$-\frac{1}{2k_0^2 n_e R_0^2} \frac{d^2 A}{d\theta^2} + V_e(\theta) A = EA, \quad (10)$$

where we have set $E \equiv (k_0^2 n_e^2 - \beta^2)/(2k_0^2 n_e)$. Let us assume an index profile $\Delta n(r, \theta)$ such that the averaged function $V_e(\theta)$ given in Eq. (6), which plays the role of a potential on the ring [see Eq. (10)], is periodic with period π , i.e., $V_e(\theta+\pi) = V_e(\theta)$, and shows two minima (double-well potential) in the interval $(0, 2\pi)$, as shown in Fig. 1. Such a situation can be realized, in practice, by assuming a step-index annular-core fiber with four core sectors with alternating refractive indices n_2 and $n_3 > n_2$, as shown in Fig. 1. In this case, the Bloch-Floquet theorem ensures that any solution to Eq. (10) has the form $A(\theta) = u_{Q,l}(\theta) \exp(iQ\theta)$ and $E = E_l(Q)$, where $-1 < Q \leq 1$, $l=1, 2, 3, \dots$, is the band index and $u_{Q,l}(\theta+\pi) = u_{Q,l}(\theta)$ is the periodic part of the Bloch function. The monodromy condition $A(\theta+2\pi) = A(\theta)$ restricts the possible values of Q to $Q=0$ or $Q=1$, yielding two sets of eigensolutions $A_l^{(e)}(\theta)$ and $A_l^{(o)}(\theta)$ with corresponding propagation constants $\beta_l^{(e)} = k_0 n_e [1 - 2E_l(0)/n_e]^{1/2} \approx k_0 n_e [1 - E_l(0)/n_e]$ and $\beta_l^{(o)} = k_0 n_e [1 - 2E_l(1)/n_e]^{1/2} \approx k_0 n_e [1 - E_l(1)/n_e]$ [see Fig. 1(c)]. Note that $A_l^{(e)}(\theta+\pi) = A_l^{(e)}(\theta)$ whereas $A_l^{(o)}(\theta+\pi) = -A_l^{(o)}(\theta)$; i.e., the two sets of modes have opposite parity (symmetric and antisymmetric modes). The two lowest-order modes $A_1^{(e)}(\theta)$ and

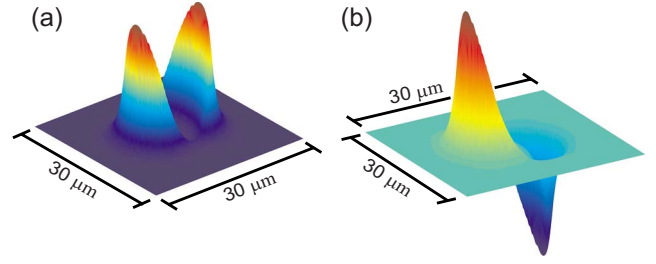


FIG. 2. (Color online) Field distribution corresponding to (a) the symmetric and (b) the antisymmetric annular fiber modes in the lowest band of Fig. 1(c).

$A_1^{(o)}(\theta)$ correspond to the usual symmetric and antisymmetric modes of the double-well potential V_e on the ring, with light localized in the two high-index regions of the annular core with different phases, as shown in Fig. 2. The splitting $\Delta\beta = \beta_0^{(e)} - \beta_0^{(o)} \approx k_0 [E_1(1) - E_1(0)]$ of their propagation constants is responsible for optical tunneling between the two high-index sectors of the annular core in such a way that an initial light beam injected in correspondence of one of the two high-index regions periodically tunnels forth and back along the propagation axial coordinate z , as will be shown by direct numerical simulations in the next section. Consider now the effect of a fiber twist. As we consider the weak guidance limit $|V_e(\theta)| \ll n_e$, one has $\beta \approx k_0 n_e$ and for a twist period $\Lambda \gg R_0$, a condition usually met in practice, the eigenvalue equation [Eq. (9)] can be simplified as follows:

$$-\frac{1}{2k_0^2 n_e R_0^2} \frac{d^2 A}{d\theta^2} + V_e(\theta) A + i \frac{\epsilon}{k_0} \frac{dA}{d\theta} = EA, \quad (11)$$

which differs from Eq. (10) for the appearance of the additional term $i(\epsilon/k_0)(dA/d\theta)$ on the left-hand side in the equation. Equation (11) can be reduced to the form (10) for the untwisted fiber after the gauge transformation $A(\theta) = \psi(\theta) \exp(i\epsilon k_0 n_e R_0^2 \theta)$, which transforms Eq. (11) into

$$-\frac{1}{2k_0^2 n_e R_0^2} \frac{d^2 \psi}{d\theta^2} + V_e(\theta) \psi = E' \psi, \quad (12)$$

with $E' = E + \epsilon^2 n_e R_0^2 / 2$. The main effect of fiber twist is thus to introduce an additional angular phase term $\exp(i\epsilon k_0 n_e R_0^2 \theta)$, whose relation with the Aharonov-Bohm phase of the corresponding quantum-mechanical problem will be clarified in the next subsection. Note that the condition of monodromy requires $\psi(\theta+2\pi) = \psi(\theta) \exp(-2\pi i \alpha)$ with

$$\alpha = \epsilon k_0 n_e R_0^2. \quad (13)$$

Therefore, writing the solution to Eq. (12) again in the Bloch-Floquet form $\psi(\theta) = u_{Q,l}(\theta) \exp(iQ\theta)$, the values of Q now allowed are given by $Q = -\alpha$ and $Q = 1 - \alpha$ for the symmetric and antisymmetric modes, and the corresponding values of propagation constants read

$$\beta_l^{(e)} \approx k_0 n_e \left[1 - \frac{E_l(-\alpha) - \epsilon^2 n_e R_0^2 / 2}{n_e} \right], \quad (14)$$

$$\beta_l^{(o)} \simeq k_0 n_e \left[1 - \frac{E_l(1-\alpha) - \epsilon^2 n_e R_0^2 / 2}{n_e} \right]. \quad (15)$$

Note that the separation $\Delta\beta_l = \beta_l^{(e)} - \beta_l^{(o)} \simeq k_0 [E_l(1-\alpha) - E_l(-\alpha)]$ of propagation constants between even and odd modes is controlled by the twist rate ϵ through the band dispersion curves E_l shown in Fig. 1(c). Note that, at values $\alpha = \pm 1/2, \pm 3/2, \pm 5/2, \dots$, one always has $E_l(-\alpha) = E_l(1-\alpha)$ owing to the symmetry of the band dispersion curves $E_l(Q)$ around $Q=0$. In such cases the propagation constants of symmetric and antisymmetric modes become degenerate, and the condition for tunneling destruction is attained. The values of spatial periods Λ of the fiber twist which correspond to tunneling suppression are thus given by $\Lambda = \Lambda_0, \Lambda_0/3, \Lambda_0/5, \dots$, where the fundamental period Λ_0 is given by

$$\Lambda_0 = \frac{8\pi^2 n_e R_0^2}{\lambda}. \quad (16)$$

Conversely, note that for $\Lambda = \Lambda_0/2, \Lambda_0/4, \dots$ one has $\alpha = 1, 2, \dots$ and therefore the twist has no effect on the tunneling dynamics.

B. Optical-quantum correspondence

To understand the physical origin of optical tunneling suppression induced by fiber twist and its connection with topological suppression of quantum tunneling on a ring threaded by a magnetic flux [4], it is worth considering the dynamics of the angular part of the light wave, as given by Eq. (8), under the paraxial approximation. After setting $f(\theta, z) = A(\theta, z) \exp(ik_0 n_e z)$ and assuming the paraxial conditions $|(\partial A / \partial z)| \ll k_0 n_e |A|$ and $|\epsilon / (k_0 n_e)| |(\partial A / \partial \theta)| \sim [1 / (k_0^2 n_e^2 R_0^2)] |(\partial^2 A / \partial \theta^2)| \sim (1/n_e) |V_e(\theta) A| \ll |A|$, from Eq. (8) the following equation of motion for the slowly varying envelope A can be derived using a multiple-scale analysis:

$$i\tilde{\lambda} \frac{\partial A}{\partial z} = -\frac{\tilde{\lambda}^2}{2n_e R_0^2} \frac{\partial^2 A}{\partial \theta^2} + V_e(\theta) A + i\tilde{\lambda} \epsilon \frac{\partial A}{\partial \theta}, \quad (17)$$

where $\tilde{\lambda} \equiv 1/k_0 = \lambda / (2\pi)$ is the reduced wavelength. In its present form, Eq. (17) is formally analogous to the quantum dynamics of a charged particle of mass $m = n_e$ and charge q on a ring of radius R_0 in the presence of an external potential $V_e(\theta)$ on the ring and threaded by a magnetic flux ϕ (see, for instance, Ref. [23]), provided that the temporal evolution of the quantum system is replaced by the spatial dynamics along the propagation axis z of the fiber and the Planck constant \hbar is replaced by the wavelength λ of the optical wave. The magnetic flux ϕ in the quantum problem is related to the fiber twist rate $\epsilon = 2\pi / \Lambda$ by the simple relation $\phi = (2\pi n_e R_0^2 \epsilon) / q$. Note that the condition for tunneling suppression at $\Lambda = \Lambda_0, \Lambda_0/3, \Lambda_0/5, \dots$ discussed in the previous subsection [see Eq. (16)] corresponds to a magnetic flux ϕ given by $\phi = \phi_0, 3\phi_0, 5\phi_0, \dots$, where $\phi_0 \equiv \lambda / (2q)$ is the analog of the elementary (two-electron) flux quantum [24]. Such a formal equivalence can be physically understood after observing that, in the transverse reference frame (r, θ) rotating

along the axis z at the twist rate ϵ , optical rays experience additional forces analogous to the centrifugal force $\mathbf{F}_{Cen} = n_e \Omega^2 r \mathbf{u}_r$, and Coriolis force $\mathbf{F}_{Cor} = 2n_e \mathbf{v} \times \Omega$, where $\Omega = \epsilon \mathbf{u}_z$ is the angular spatial frequency of the twist (see, for instance, Ref. [18]). In terms of wave optics description, the effect of the centrifugal force on the ring is merely to shift the eigenvalue (energy) E to E' by the centrifugal potential term $-(1/2)\Omega^2 n_e R_0^2$ [see Eq. (12)], whereas the Coriolis force is equivalent to the magnetic (Lorentz) force experienced by a particle of charge q in a uniform magnetic field $\mathbf{B} = (2n_e / q) \Omega = (2n_e \epsilon / q) \mathbf{u}_z$ and is thus expected to introduce a topological (Aharonov-Bohm) phase term in the optical wave function. In fact, the motion of a quantum particle in the presence of a magnetic flux along a closed path, such as along a ring of radius R_0 , leads to an additional Aharonov-Bohm phase term $\exp(\pm i q \phi / \hbar) = \exp(\pm 2\pi i \alpha)$, where $\phi = \pi R_0^2 B$ is the magnetic flux (see, for instance, Ref. [9]). Taking into account that $B = 2n_e \epsilon / q$, the Aharonov-Bohm phase term then reads $\exp(\pm i \pi \phi / \phi_0) = \exp(\pm i \pi \Lambda_0 / \Lambda)$, where Λ_0 is defined by Eq. (16). Quenching of tunneling splitting then corresponds to the values $\pi, 3\pi, 5\pi, \dots$, of the Aharonov-Bohm phase, at which a destructive interference between the two different tunneling paths occurs [4].

IV. NUMERICAL RESULTS

We checked the occurrence of topological tunneling suppression by a direct beam propagation analysis of light waves in a step-index annular-core fiber made of four sectors, as shown in Fig. 1(a). Geometrical and optical parameters of the fiber used in the numerical simulations are $a = 7 \mu\text{m}$, $\delta = 1 \mu\text{m}$, $n_s = 1.45067$, $n_2 - n_s = 0.02$, $n_3 - n_s = 0.022$, and $\lambda = 980 \text{ nm}$ and refer to a cladding region made of fused silica. The index changes $(n_2 - n_s)$ and $(n_3 - n_s)$ in the core regions can be achieved, for instance, by GeO_2 doping with concentrations of about 16% / mol for $(n_2 - n_s)$ and 18% / mol for $(n_3 - n_s)$ [25]. The modes and corresponding propagation constants of the untwisted fiber were first determined numerically by a standard mode-solver technique. The profiles of the two lowest-order modes, corresponding to the symmetric and antisymmetric functions $A^{(e)}(\theta)$ and $A^{(o)}(\theta)$ on the ring discussed in Sec. III A, are depicted in Fig. 2. The separation $\Delta\beta$ of their propagation constants turns out to be $\Delta\beta \simeq 0.178 \text{ mm}^{-1}$, which corresponds to a spatial tunneling period $z_T = 2\pi / \Delta\beta \simeq 35.3 \text{ mm}$. The fundamental period Λ_0 of fiber twist corresponding to tunneling quenching, as calculated using Eq. (16) with a numerically computed $R_0 \simeq 6.5 \mu\text{m}$ effective ring radius [see Eq. (7)], turns out to be $\Lambda_0 \simeq 4.94 \text{ mm}$. To study beam propagation along the fiber, we numerically integrated Eq. (1) using a standard beam propagation method (BPM) on a square $30 \mu\text{m} \times 30 \mu\text{m}$ integration domain with 256×256 spectral modes and with absorbing boundary conditions. Integration has been performed along the forward propagation direction in the twisted reference frame neglecting backscattered waves. Note that the use of a simple one-directional BPM technique rather than a bidirectional BPM is justified in our case because we just consider twist periods Λ much longer than the

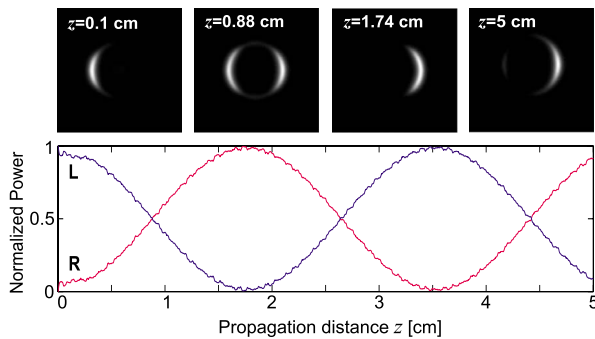


FIG. 3. (Color online) Numerically computed fractional beam power trapped in the left (L) and right (R) fiber sectors versus propagation distance z in a $L=5$ cm long untwisted annular fiber excited by an elliptical Gaussian beam on the left sector, showing periodic optical tunneling between left and right high-index core sectors. The top images show the transverse field intensity distribution at a few propagation distances in a gray scale plot.

wavelength λ , whereas the scalar approximation is consistent with the small index change between cladding and core regions. As an initial condition at the $z=0$ input plane, we assumed an elliptical Gaussian beam with spot size [full width at half maximum (FWHM)] $w_x=3 \mu\text{m}$ and $w_y=12 \mu\text{m}$, centered in one of the two high-index sectors of the annular core. Figure 3 shows the numerically computed fractional beam powers trapped in the right (R) and left (L) sectors of the fiber for $\Lambda=\infty$ (untwisted fiber) and for a propagation distance up to $L=5$ cm, together with the detailed images of transverse intensity profiles at a few propagation distances. Note the characteristic oscillation of the beam power (optical tunneling) between the two sectors with a spatial period very close to the theoretical value $z_T \approx 35.3$ mm. For the sake of clearness, in the figure at each propagation distance z the power in the two sectors has been normalized to the total beam power trapped in the whole integration domain at the same propagation distance, so that radiation losses (simulated by the absorbing boundary conditions) are not included in the figure [26]. Figures 4–6 show

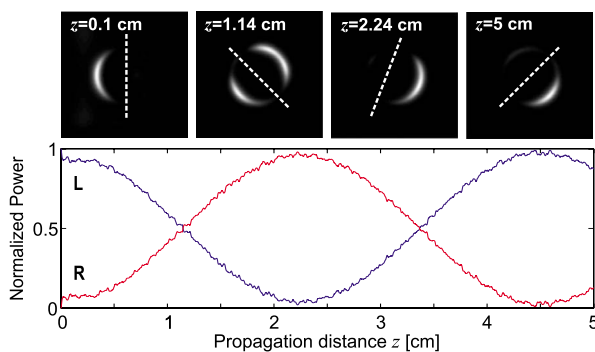


FIG. 4. (Color online) Same as Fig. 3, but for a twisted fiber with a twist period $\Lambda=2\Lambda_0=9.88$ mm. The transverse field intensity distributions in the top images are taken in the laboratory (nonrotating) reference frame (x,y) . The dotted lines in the four images show the local position of the fiber Y axis [see Fig. 1(a)] which rotates along the propagation distance.

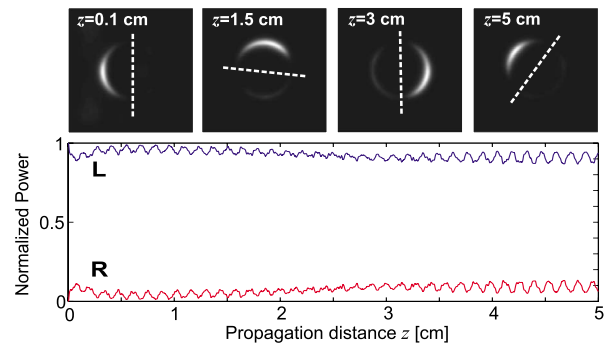


FIG. 5. (Color online) Same as Fig. 3, but for a twist period $\Lambda=\Lambda_0=4.94$ mm, corresponding to topological suppression of optical tunneling.

the behavior of the fractional beam power trapped in the two fiber sectors for increasing values of the twist rate $\epsilon=2\pi/\Lambda$ at $\Lambda=2\Lambda_0$, $\Lambda=\Lambda_0$, and $\Lambda=\Lambda_0/2$. Note that, according to the theoretical predictions of Sec. III, as ϵ increases from zero the tunneling period first increases (Fig. 4) up to $\epsilon=2\pi/\Lambda_0$, where tunneling is almost suppressed (Fig. 5). As ϵ is further increased, the tunneling period decreases up to $\epsilon=\pi/\Lambda_0$ (Fig. 6), where the dynamical scenario of the untwisted fiber is basically retrieved.

V. CONCLUSIONS

In this work we have theoretically proposed a fiber-optics analog of topological suppression of quantum tunneling in a double-well system on a ring. Propagation of light waves in a twisted annular fiber with a structured core has been shown to mimic the temporal dynamics of a charged particle in a double-well potential on a ring threaded by a magnetic field, for which a topological suppression of tunneling is possible at certain values of the magnetic flux [4]. Numerical simulations performed for an annular-core fiber made by four sectors with alternating high and low refractive index have confirmed the occurrence of topological tunneling suppression at special values of the fiber twist rate. The phenomenon of topological tunneling suppression can be of course extended to other fiber geometries, provided that the light path in the core forms a closed loop and two optical trapping regions

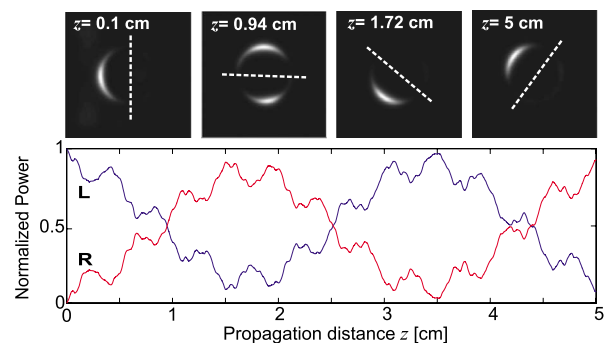


FIG. 6. (Color online) Same as Fig. 3, but for a twist period $\Lambda=\Lambda_0/2=2.47$ mm.

exist along the path. Such a situation can be found, for instance, in an elliptical annular core fiber with an unstructured core, where the ellipticity of the annular core induces an effective double-well potential for the light waves analogously to what happens for matter waves in elliptically shaped optical ring traps [27]. It should be finally noted that the proposed optical-quantum analogy, besides for providing a novel example in classical wave optics of Aharonov-Bohm interference of quantum mechanics, is rather distinct from the optical realization of CDT in a driven double well on a

line [2,3] recently observed in a periodically curved optical directional coupler [14]. In fact, as CDT is associated with quasienergy crossing of the periodically driven double-well system and in the optical system of Ref. [14] this was realized by spatially shaking the double-well potential, suppression of tunneling in the twisted annular fiber is due to a destructive interference between two different tunneling paths [4,8] and is controlled by the additional topological phase induced by the fiber twist which is the optical analog of the Aharonov-Bohm phase.

-
- [1] M. Razavy, *Quantum Theory of Tunneling* (World Scientific, River Edge, NJ, 2003).
- [2] M. Grifoni and P. Hänggi, *Phys. Rep.* **304**, 229 (1998).
- [3] F. Grossmann, T. Dittrich, P. Jung, and P. Hänggi, *Phys. Rev. Lett.* **67**, 516 (1991); F. Grossmann, P. Jung, T. Dittrich, and P. Hänggi, *Z. Phys. B: Condens. Matter* **84**, 315 (1991).
- [4] S. Weigert, *Phys. Rev. A* **50**, 4572 (1994).
- [5] D. Loss, D. P. DiVincenzo, and G. Grinstein, *Phys. Rev. Lett.* **69**, 3232 (1992).
- [6] A. Garg, *Europhys. Lett.* **22**, 205 (1993).
- [7] W. Wernsdorfer and R. Sessoli, *Science* **284**, 133 (1999).
- [8] S. Weigert, *Phys. Rev. Lett.* **75**, 1435 (1995).
- [9] J. H. Harris and M. D. Semon, *Found. Phys.* **10**, 151 (1980).
- [10] D. Dragoman and M. Dragoman, *Quantum-Classical Analogies* (Springer, Berlin, 2004).
- [11] R. J. Black and A. Ankiewicz, *Am. J. Phys.* **53**, 554 (1985).
- [12] S. Longhi, D. Janner, M. Marano, and P. Laporta, *Phys. Rev. E* **67**, 036601 (2003).
- [13] I. Vorobeichik, E. Narevicius, G. Rosenblum, M. Orenstein, and N. Moiseyev, *Phys. Rev. Lett.* **90**, 176806 (2003).
- [14] G. Della Valle, M. Ornigotti, E. Cianci, V. Foglietti, P. Laporta, and S. Longhi, *Phys. Rev. Lett.* **98**, 263601 (2007).
- [15] P. St. J. Russell, *J. Lightwave Technol.* **24**, 4729 (2006).
- [16] M. Bayindir, A. F. Abouraddy, O. Shapira, J. Viens, D. Saygin-Hinczewski, F. Sorin, J. Arnold, J. D. Joannopoulos, and Y. Fink, *IEEE J. Sel. Top. Quantum Electron.* **12**, 1202 (2006).
- [17] A. Zoubir, A. Cedric Lopez, M. Richardson, and K. Richardson, *Opt. Lett.* **29**, 1840 (2004).
- [18] S. Longhi, G. Della Valle, and D. Janner, *Phys. Rev. E* **69**, 056608 (2004).
- [19] R. H. Stolen, *Appl. Opt.* **14**, 1533 (1975).
- [20] B. C. Sarkar, P. K. Choudhury, and T. Yoshino, *Microwave Opt. Technol. Lett.* **31**, 435 (2001); J. Marcou and S. Fevrier, *Microwave Opt. Technol. Lett.* **38**, 249 (2003).
- [21] M. Hautakorpi and M. Kaivola, *J. Opt. Soc. Am. A* **22**, 1163 (2005).
- [22] Reduction of the dynamics to the angular ring coordinate is commonplace in many problems dealing with mesoscopic electron or matter wave transport on a ring [see, for instance, H. Saito and M. Ueda, *Phys. Rev. Lett.* **93**, 220402 (2004); see also Ref. [23]].
- [23] S.-L. Zhu, *Solid State Commun.* **113**, 233 (2000).
- [24] The values $\phi = \phi_0, 3\phi_0, 5\phi_0, \dots$ of magnetic flux leading to tunneling suppression have been obtained in Ref. [4] using a path integral analysis [see in particular Eq. (41) of Ref. [4]].
- [25] H. Murata, *Handbook of Optical Fibers and Cables* (Marcel Dekker, New York, 1996), p. 18.
- [26] Radiation losses are mainly due to mode mismatching at the input fiber section. For a propagation length $L=5$ cm, numerically computed radiation losses turn out to be $\sim 54\%$ for the untwisted fiber and slightly larger for the twisted fibers.
- [27] S. Schwartz, M. Cozzini, C. Menotti, I. Carusotto, P. Bouyer, and S. Stringari, *New J. Phys.* **8**, 162 (2006).